

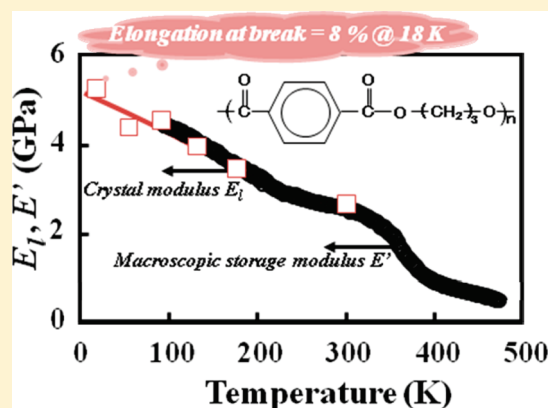
## Cryogenic Mechanical Behavior of Poly(trimethylene terephthalate)

Takashi Nishino,\* Tai'ichi Okamoto, and Hiroshi Sakurai

Department of Chemical Science and Engineering, Graduate School of Engineering, Kobe University, Rokko, Nada, Kobe 657-8501, Japan

Supporting Information

**ABSTRACT:** Tensile deformation behaviors of the crystalline regions of poly(trimethylene terephthalate) (PTT) and of PTT films were investigated at temperatures ranging from room temperature down to 18 K. The elastic moduli of the crystalline regions (crystal modulus) were found to be temperature dependent. Measured by X-ray diffraction, the crystal modulus along the chain axis ( $E_l$ ) was 2.59 GPa at 300 K and 5.39 GPa at 18 K, and the crystal modulus in the direction perpendicular to the chain axis ( $E_t$ ) was 3.7 GPa at 300 K and 7.4 GPa at 18 K. This inversion of the usual order of  $E_l$  and  $E_t$  values is a result of the extraordinarily small  $E_l$  due to the very contracted skeleton of PTT and makes a PTT film macroscopically isotropic even after uniaxial drawing up to a draw ratio of 4. The  $E_l$  and the macroscopic storage modulus coincide each other, and both increased with decreasing temperature. Even at 18 K, a drawn PTT film could be strained up to 8% without loading–unloading hysteresis.



## INTRODUCTION

The Young's moduli of polymeric materials at room temperature range over 7 orders of magnitude, from kilopascals for elastomers and gels to hundreds of gigapascals for ultrahigh-modulus polymers,<sup>1</sup> and the design freedom provided by this wide range is one of the reasons polymers find so many applications in industry as well as our daily lives. High elasticity is one of the peculiar mechanical properties of polymers,<sup>2</sup> and the polymers called elastomers or rubbers can be reversely elongated to several hundred percent of their original length. Many of the polymers used for sealing and packing and many of the polymers used in nuclear reactors and in aerospace, nuclear industries need to be highly elastic even at very low temperatures.<sup>3</sup> Though tensile strength and Young's modulus usually increase as temperature is decreased, at cryogenic temperatures—that is, temperatures like those of liquid nitrogen (75 K) and liquid helium (4 K)—most polymers, even elastomers, become so brittle and fragile that they can be elongated no more than 3% before breaking. The high elasticity of an elastomer above its glass transition temperature  $T_g$  is mostly an entropy elasticity due to vigorous micro-Brownian motions of the polymer chains, and the lowest  $T_g$  reported for a polymer is the 134 K reported for poly(diethyl siloxane).<sup>4</sup> This would mean that all polymers would be glassy because the high elasticity based on entropy elasticity is diminished at cryogenic temperatures, which tends to limit the usage of polymeric materials. An alternative way of achieving cryogenic small Young's modulus and high elasticity is expected to be by utilizing energy elasticity of some polymers.

The elastic moduli of the crystalline regions are among the most important mechanical properties of polymers, and for a

variety of polymers, the elastic modulus in the direction parallel to the chain axis (*i.e.*, the crystal modulus  $E_l$ ) has been measured by X-ray diffraction.<sup>5–9</sup> As the  $E_l$  of a polymer depends only on the energy elasticity, thus an oriented polymer with a very small  $E_l$  would be likely to have a very low macroscopic modulus of elasticity even at cryogenic temperatures.

Poly(trimethylene terephthalate) (PTT) is a member of the series of aromatic polyesters in which the number of methylene units in the main chain is between that in poly(ethylene terephthalate) (PET) and that in poly(butylene terephthalate) (PBT). PTT has been known for many years but commercialized only recently because 1,3-propylene glycol has been obtained from starch economically and ecologically by using a fermentation process.<sup>10</sup> PTT is well-known to have a small elastic modulus and show excellent elastic recovery.<sup>11</sup> Its large crystal elongation under macroscopic stretching, and easy relaxation after removal of stretching were first reported by Jakeways and Ward,<sup>12,13</sup> and Wu et al. found that its crystal strain in the chain direction could be as much as 5.6%.<sup>14</sup> We reported the  $E_l$  of PTT to be only 2.59 GPa at room temperature: the smallest room-temperature  $E_l$  reported for a polymer.<sup>15</sup> Another interesting and unique feature of PTT is that at room temperature its  $E_l$  is smaller than the elastic modulus  $E_t$  in the direction perpendicular to the chain axis (3.7 GPa).<sup>15</sup> This means that in PTT it is easier to elongate the skeletal chains themselves than it is to increase the intermolecular distance in the crystal lattice. Accordingly, PTT is

Received: January 17, 2011

Revised: February 14, 2011

Published: March 04, 2011

expected to have a very small Young's modulus and show high elasticity even at cryogenic temperatures.

Investigating the crystal modulus at cryogenic temperatures is also important because  $E_l$  provides us with information about the molecular skeleton and molecular deformation mechanisms in the crystal lattice. We have previously measured the  $E_l$  of polymers at high and low temperatures and for each polymer have discussed those  $E_l$  values in terms of the thermal molecular motions in the crystalline regions. The results of our past investigations revealed that the  $E_l$  values for atactic poly(vinyl alcohol),<sup>16</sup> PBT  $\alpha$ -form,<sup>17</sup> nylon-6<sup>18</sup> are temperature dependent and that the crystal lattices in these polymers are influenced by incoherent thermal molecular motions in the crystalline regions. Therefore, to obtain information on the crystal modulus purely based on the energy elasticity of polymer crystal (*i.e.*, to exclude the thermal effects), we should measure the  $E_l$  at very low temperatures. These measured  $E_l$  values are also useful for comparison with the calculated values because most calculations of the crystal modulus neglect incoherent thermal effects.<sup>19</sup> The temperature of liquid nitrogen is well below  $T_g$  of any polymer but is above the temperature of the  $\gamma$  relaxation, in which the molecular motions in the crystal lattice are reported take part.<sup>20,21</sup>

In this study we measured the  $E_l$  and  $E_t$  of PTT at temperatures down to 18 K, investigated the cryogenic macroscopic mechanical behaviors of the uniaxially and biaxially drawn PTT films, and compared the macroscopic deformation with the crystal lattice one.

## EXPERIMENTAL SECTION

**Materials.** PTT pellets (Asahi Kasei Chemicals, PTT-BR) were dried for 3 h at 393 K, hot-pressed at 423 K, and then quenched in ice–water. The quenched films had an intrinsic viscosity number of 0.92, corresponding a weight-average molecular weight of  $33 \times 10^3$ ,<sup>22</sup> and a titanium oxide content below 0.05 wt %. The films were uniaxially drawn at 343 K to a draw ratio  $\lambda$ . Unless otherwise mentioned,  $\lambda = 4$  for all of the films investigated in the work reported here. Some of the drawn films were annealed for 30 min at 473 K at the constant length. For comparison, a quenched PET film was drawn ( $\lambda = 4$ ) at 378 K and then annealed for 45 min at 493 K.

A quenched film 30 mm square was also simultaneously biaxially drawn at 3 mm/min to  $\lambda = 3$  at 323 K by using a biaxial stretching system (Shibayama Scientific Co. Ltd., SS-60).

**Characterizations.** The density  $d$  of the specimen was measured at 303 K by the floatation method, using benzene and carbon tetrachloride, and the crystallinity  $X_c$  of the sample was calculated as follows:

$$(1/d) = (X_c/d_c) + (1 - X_c)/d_a \quad (1)$$

where  $d_c$  is the crystal density ( $1.432 \text{ g/cm}^3$ )<sup>23</sup> and  $d_a$  is the amorphous density ( $1.307 \text{ g/cm}^3$ ).<sup>24</sup>

X-ray diffraction photographs were recorded on an imaging plate having a camera length of 37.5 mm. The specimen was irradiated perpendicular to the fiber axis with the Cu K $\alpha$  radiation generated by a Rigaku RINT-2000 operating at 40 kV and 20 mA.

The melting temperature  $T_m$  of a film sample was identified as the temperature of the endothermic peak in the thermogram obtained when the sample was heated at 10 K/min under nitrogen flow in a differential scanning calorimeter (Seiko Instruments, DSC-220).

The dynamic viscoelastic properties of samples (original length = 10 mm) were measured, in a nitrogen atmosphere, using a DVA-220S dynamic mechanical analyzer (ITK Ltd.), at a heating rate of 6 K/min, and a frequency of 10 Hz. A tensile deformation of 0.25% was applied to

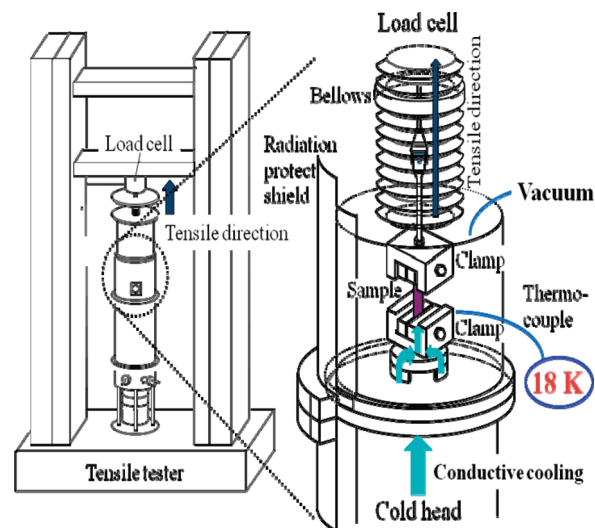


**Figure 1.** Schematic illustration of setup for tensile tests at cryogenic temperatures.

the sample, and the temperature of the most intense relaxation peak on the  $\tan \delta$  versus temperature curve was defined as  $T_g$ .

The stress–strain curves of 200- $\mu\text{m}$ -thick samples 5 mm wide and originally 20 mm long were measured at an extension rate of 1 mm/min by using an Autograph AGS-1kND tensile tester (Shimadzu). The cross-section was prepared by cutting the film with a glass knife in the direction normal to the sample surface, and the cross-sectional area was evaluated from the density, the weight, and the length of the sample. The means and standard deviations were calculated for the macroscopic specimen modulus  $Y_b$ , tensile strength, and elongation at break measured for five samples. The angular dependence of the specimen Young's modulus  $Y_\theta$  was measured by cutting the rectangular specimen at the angle  $\theta$  to the draw direction.

**Cryogenic Measurements.** The crystal modulus of a polymer at cryogenic temperatures should be evaluated by using X-ray diffraction to measure the change in the lattice spacing under a constant stress. A stretching device and a load cell were therefore combined with a cryostat cell and mounted on an X-ray goniometer.<sup>8</sup> The film sample was clamped to the stretching device under vacuum and cooled by thermal conduction via the clamp closest to the cold head. The sample was subjected to a constant stress  $\sigma$  and the change in the lattice spacing for the designated reflection (*i.e.*, the strain  $\varepsilon$  in the corresponding direction) was measured in a symmetrical transmission geometry using Cu K $\alpha$  radiation. The  $E_l$  and  $E_t$  were calculated under the assumption of a homogeneous stress distribution as follows:

$$E_l, E_t = \sigma/\varepsilon \quad (2)$$

The stress–strain curve of the crystal lattice was obtained by increasing the stress successively, and the crystal modulus was evaluated from the inclination of that curve. This evaluation procedure is described in more detail in earlier papers.<sup>5–9</sup>

For measuring the macroscopic stress–strain curve at cryogenic temperature, cryogenic system was combined with a conventional Instron type tensile tester. As shown schematically in Figure 1, the film sample was clamped and cooled by thermal conduction via the bottom clamp from the cold head. In this case, the clumped specimen was tensile tested from the outside of the cryostat through a bellows, and the stress was detected by the load cell. The original length and the tensile speed were identical to those employed at room temperature. Cyclic tests were performed by repeatedly increasing and releasing the applied strain.

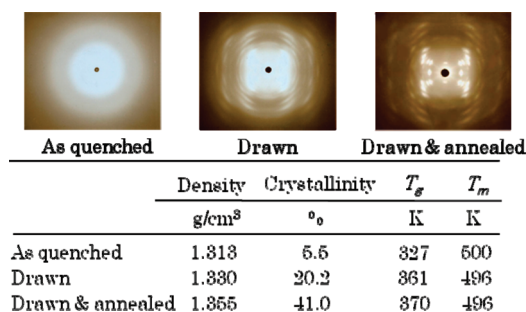


Figure 2. X-ray diffraction photographs, density, crystallinity, and thermal properties of variously treated PTT films.

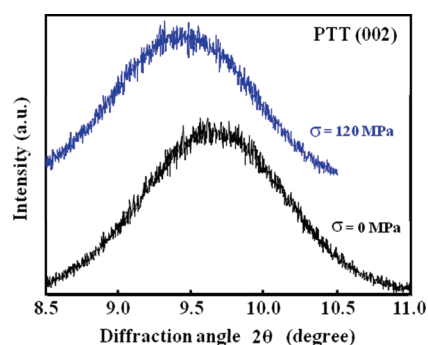


Figure 3. X-ray diffraction profiles for the (002) plane of a drawn-and-annealed PTT film before loading and under loading at 18 K.

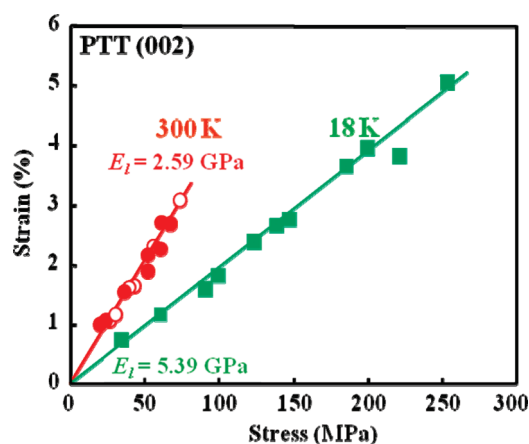


Figure 4. Stress-strain curves for the (002) plane of drawn-and-annealed PTT films at (■) 18 K and at (○) 300 K. Also shown are the plots for drawn PTT films at 300 K (●).

## RESULTS AND DISCUSSION

X-ray diffraction photographs and the density, crystallinity,  $T_g$ , and  $T_m$  of the variously treated PTT films are shown in Figure 2. As-quenched films showed a diffuse halo in the X-ray diffraction photograph, so even though the crystallization rate of PTT is in an order of magnitude faster than that of PET,<sup>25</sup> the as-quenched films were in an almost amorphous state with very low crystallinity. Both drawing and annealing increased the crystallinity of the PTT, and the resultant increases in crystallinity were accompanied by increases of  $T_g$ . The reflection used for measuring the  $E_l$  was the 002 reflection, which in the X-ray diffraction photograph of the drawn-and-annealed film clearly appeared at

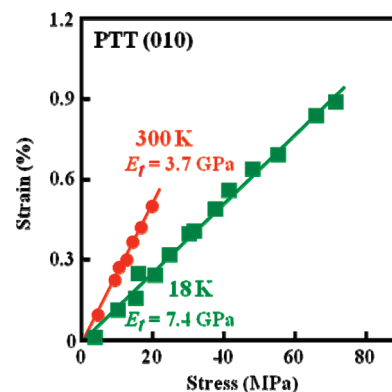


Figure 5. Stress-strain curves for the (010) plane of drawn-and-annealed PTT films at (■) 18 K and (●) 300 K.

the meridian. A lot has been reported on the crystal structure of PTT,<sup>23,26–30</sup> and according to Tadokoro et al. the crystal system of PTT is a triclinic system with  $a = 4.58 \text{ \AA}$ ,  $b = 6.22 \text{ \AA}$ ,  $c = 18.12 \text{ \AA}$ ,  $\alpha = 96.9^\circ$ ,  $\beta = 89.4^\circ$ , and  $\gamma = 111.0^\circ$ . The normal of the (002) plane should therefore be inclined  $7.2^\circ$  to the fiber axis. As seen in the Supporting Information, Figure S1, however, the intensity maximum of this reflection was in precisely the meridional direction. This reveals that the crystallites in the fiber are tilted slightly, which is not unusual for aromatic polyesters.<sup>31</sup>

Figure 3 shows the X-ray diffraction profiles for the 002 reflection of a drawn-and-annealed PTT film before and while being subjected to 120-MPa stress at 18 K. The constant stress shifted the diffraction peak to a lower angle. This indicates that the 002 spacing, and thus the skeleton of PTT molecule, was elongated in the stress direction. The experimental error in measuring the peak shift due to the lattice extension was ordinarily less than  $0.01^\circ$  in angle  $2\theta$ , which corresponds to a lattice strain of 0.1%.

Figure 4 shows the stress-strain curves for the (002) plane of PTT at 18 and 300 K, where one sees that at 300 K the plots for the drawn film (crystallinity  $\chi_c = 20.2\%$ ) and those for the drawn-and-annealed film ( $\chi_c = 41\%$ ) coincide within experimental error. The inclination of the line through those plots corresponds to an  $E_l$  of 2.59 GPa, which is the same as the  $E_l$  previously reported for a drawn and annealed PTT fiber.<sup>15</sup> Although the drawn and the drawn-and-annealed films have different microstructures, the identity of their  $E_l$  values is strong evidence that the stress distribution in PTT is homogeneous. At 18 K lattice extension up to 5% was reversible and the measured strain plotted against stress give a straight line through the origin, the slope of which corresponds to an  $E_l$  of 5.39 GPa, more than twice the  $E_l$  of PTT at 300 K. This indicates that the  $E_l$  value of PTT is temperature dependent at lower temperature region.

The  $E_l$  of PET, on the other hand, a polymer differing from PTT by only one methylene group per monomer, is 108 GPa at 300 K and remains unchanged at temperatures up to 473 K.<sup>32</sup> The  $E_l$  values we report here for PTT are the lowest for polymers we have investigated.

Figure 5 shows the stress-strain curves for the equatorial (010) plane of PTT at 18 and 300 K. The lattice extensions were reversible, and the slopes of the lines in Figure 5 give  $E_l$  values of 3.7 GPa at 300 K and 7.4 GPa at 18 K. These values are comparable to the value calculated by molecular mechanics (9.2 GPa)<sup>33</sup> and the observed sonic modulus for the crystalline regions (4.15 GPa).<sup>34</sup> Reflecting the high anisotropy of polymer



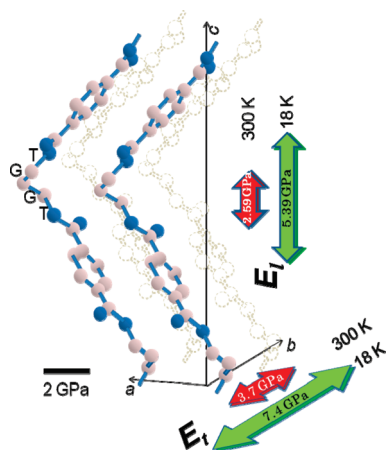


Figure 6. Crystal structure of PTT<sup>30</sup> with the anisotropy of the crystal modulus  $E_l$  and  $E_t$  values at 18 and 300 K.

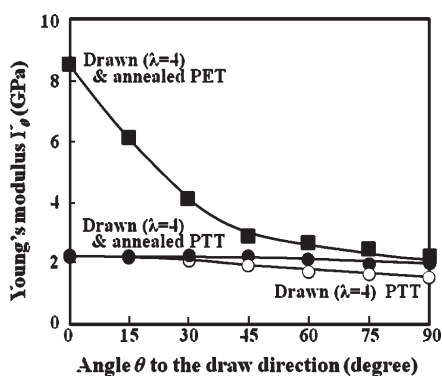


Figure 7. Relationship between Young's modulus  $Y_\theta$  at 300 K and the angle  $\theta$  to the draw direction for (○) drawn PTT, (●) drawn-and-annealed PTT, and that for (■) drawn-and-annealed PET.

crystals, the arrangement of covalent bonds along polymer chains, and vice-valent interaction between chain molecules, the  $E_t$  is much smaller than the  $E_l$  for all polymers except PTT. On the contrary, for PTT, this usual order of the sizes of the  $E_l$  and the  $E_t$  is reversed at cryogenic temperatures as well as at room temperature.

Figure 6 shows the skeletal structure of PTT in the crystal lattice drawn after Yang et al.<sup>30</sup> The skeleton of PTT draws large zigzag structure through the internal rotation around the single bonds at the methylene units with trans-gauche-gauche-trans conformation. Comparing the fiber identity period—i.e.,  $c$ -axis dimension (18.12 Å)—with the identity period for the fully extended skeleton ( $c = 24.16$  Å), shows that the chain is contracted by 25%. Applying a tensile force to this molecule, together with stretching of the bonds themselves and bending of the bond angles, the chain are mainly deformed by the internal rotations around the methylene units, whose force constants are very low. This is why the crystal modulus of PTT is very small even at cryogenic temperatures. The reported unit cell dimensions for the  $c$ -axis of PTT are scattered between 18.12 and 18.61 Å,<sup>23,26–30</sup> perhaps because the small  $E_l$  of PTT caused the residual stress of the specimens used for structural analyses to vary between laboratories.

The normal of the (010) plane is parallel to the direction in which intermolecular dipole–dipole interaction of ester groups

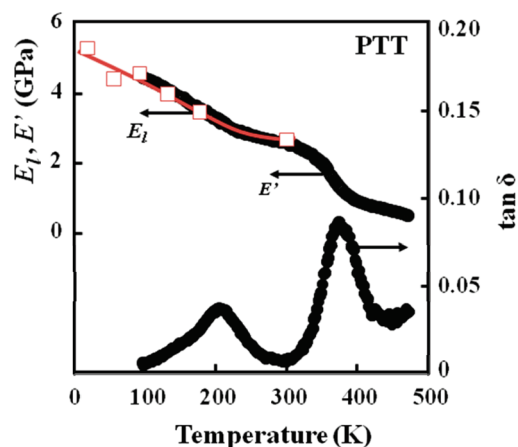


Figure 8. Temperature dependences of the (□) crystal modulus  $E_b$  (○) dynamic storage modulus  $E'$ , and (●) loss tangent ( $\tan \delta$ ) of drawn PTT films ( $\lambda = 4$ ).

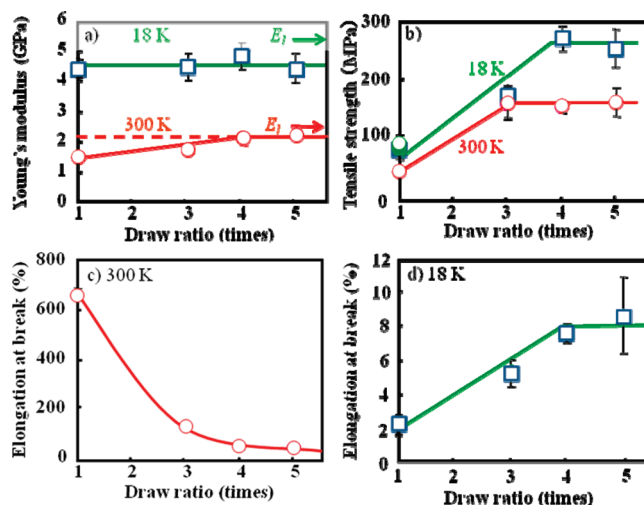


Figure 9. Relationships between draw ratio and (a) the Young's modulus of drawn PTT at 300 and 18 K, (b) the tensile strength of drawn PTT at 300 and 18 K, (c) the elongation at break of drawn PTT at 300 K, and (d) the elongation at break of drawn PTT at 18 K.

acts. At room temperature the  $E_t$  of PET is 4.1 GPa<sup>35</sup> and the  $E_t$  of PBT $\alpha$ -form is 2.2 GPa.<sup>36</sup> The  $E_t$  of PTT at 300 K, 3.7 GPa, is between those values, which is reasonable when one considers the effect of the number of methylene units (i.e., the ester-group density). Accordingly, the observed reversal of the usual order of the sizes of the  $E_l$  and the  $E_t$  is due to the extraordinarily small  $E_l$  of PTT.

Figure 7 shows the relationship between the  $Y_\theta$  at 300 K and the angle to the draw direction for the drawn and the drawn-and-annealed PTT films and that for the drawn-and-annealed PET film. The drawn-and-annealed PET film showed large anisotropy of the  $Y_\theta$  value depending on the angle  $\theta$ , which is commonly observed for most polymers. The reversal of the usual order of the sizes of the  $E_l$  and the  $E_t$  might be expected to cause  $Y_\theta$  to increase with the angle  $\theta$ , but such behavior was not seen. The  $Y_\theta$  for the drawn PTT film decreased slightly with increasing  $\theta$ , and the  $Y_\theta$  for the drawn-and-annealed PTT film was almost constant:  $2.1 \pm 0.1$  GPa. This mechanical isotropy is unique to PTT even though polymer chains are highly oriented in the draw direction.

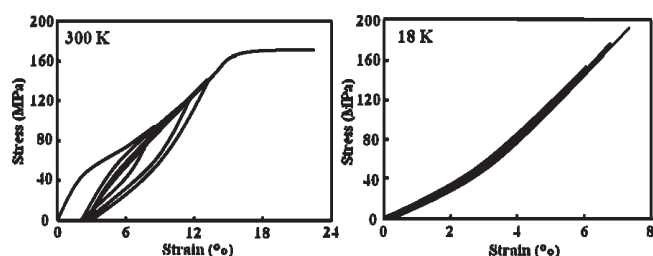


Figure 10. Stress–strain curves of drawn PTT films ( $\lambda = 4$ ) under cyclic loads at 300 and 18 K.

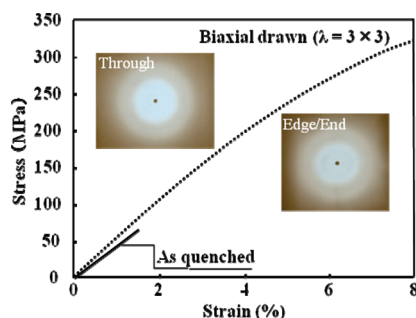


Figure 11. Stress–strain curves of as-quenched and biaxially drawn PTT films at 18 K.

Figure 8 shows the temperature dependence of the storage modulus  $E'$  and mechanical  $\tan \delta$  of drawn PTT films ( $\lambda = 4$ ), where the temperature dependence of the  $E_t$  is also shown by square plots (the stress–strain curves of the crystal lattice at each temperature are shown in the Supporting Information, Figure S2). The  $E_t$  changed gradually with temperature, which reveals that the skeleton of PTT is easily influenced by the thermal motions of extraordinary flexible molecules in the crystalline regions. Both the  $E_t$  and the  $E'$  increased with decreasing temperature, and this indicates that the macroscopic deformation of PTT is highly governed by the crystal-like one even though the  $X_c$  value does not reach 100%. This is because the small  $E_t$  of PTT acts in concert with the increase of the modulus of the amorphous region at lower temperatures.

Figure 9 shows the relationships between the draw ratio and the macroscopic Young's modulus  $Y_t$ , tensile strength, and elongation at break of drawn PTT films at 18 and 300 K. At 300 K the  $Y_t$  increased slightly with the draw ratio, but at 18 K it remained unchanged; independent of the draw ratio. At both temperatures the  $Y_t$  values were more than 85% of the  $E_t$  values. The tensile strength increased greatly with increasing draw ratio. This shows that the chain orientation mainly gives an effect on the increase of tensile strength, but not on the  $Y_t$  value. At 300 K the elongation at break decreased with draw ratio, but at 18 K it increased with draw ratio and reached 8%. This elongation is very large because for most materials at cryogenic temperatures the elongation at break is less than 3%.<sup>3</sup>

Figure 10 shows the stress–macroscopic strain curves of drawn PTT films under cyclic loads at 300 and 18 K. The loading and unloading curves obtained at 300 K show hysteresis loops, but those obtained at 18 K coincide with one another up to 8%. Yano and Yamaoka reported that the elongation at break of some polyimides is more than 10% at 77 K.<sup>20</sup> However, polyimides deformed with yielding at the strain less than 5%, after which plastic deformation was observed. Accordingly, to the best of our

knowledge, PTT is the only polymer possessing high elasticity up to 8% based on energy elasticity at 18 K.

Figure 11 shows the stress–macroscopic strain curves of as-quenched and quenched-and-biaxially drawn ( $\lambda = 3$ ) PTT films at 18 K. The crystallinity of the biaxially drawn film was 20%, identical to that of a film drawn uniaxially to  $\lambda = 3$ . The X-ray diffraction photographs showed that the crystallites in the biaxially drawn film were randomly oriented in both through and edge/end directions. Both the tensile strength and elongation at break were increased by biaxial drawing, reaching values as high as 265 MPa and 8%. Biaxial drawing was found to greatly increase the toughness of PTT at cryogenic temperatures.

## CONCLUSIONS

The crystal moduli  $E_t$  and  $E_c$  of PTT are temperature dependent, and below room temperature it is harder to increase the intermolecular distance than it is to elongate those chains themselves in the PTT crystal lattice. This reversal of the usual order of the  $E_t$  and the  $E_c$  is a result of the extraordinarily small  $E_t$  due to the contracted skeleton of PTT and makes a PTT film macroscopically isotropic even after uniaxial drawing to  $\lambda = 4$ . With decreasing temperature both the storage modulus  $E'$  and the  $E_t$  increased. The macroscopic deformation of drawn PTT at cryogenic temperatures was found to be determined by the crystal deformation, in other words, by energy elasticity. Even at 18 K, both uniaxially and biaxially drawn PTT films could be strained up to 8% without loading–unloading hysteresis, and this is the largest reported elastic deformation at a cryogenic temperature.

## ASSOCIATED CONTENT

**S Supporting Information.** Figure S1, showing the diffraction intensity versus the angle of inclination to the (002) plane for (a) drawn and (b) drawn-and-annealed PTT films, and Figure S2 showing the stress–strain curves for the (002) plane of drawn-and-annealed PTT films at various temperatures. This material is available free of charge via the Internet at <http://pubs.acs.org>.

## AUTHOR INFORMATION

### Corresponding Author

\*Telephone: +81-78-803-6164. Fax: +81-78-803-6198. E-mail: [tnishino@kobe-u.ac.jp](mailto:tnishino@kobe-u.ac.jp).

## ACKNOWLEDGMENT

The authors thank the financial support by a Grant-on-Aid for Scientific Research from the Ministry of Education, Culture, Science, Sports and Technology, Japan (No. 20246100). Special Coordination Funds for Promoting Science and Technology, Creation of Innovation Centers for Advanced Interdisciplinary Research Areas (Innovative Bioproduction Kobe), MEXT, Japan, are also acknowledged.

## REFERENCES

- (1) Ward, I. M. *Mechanical Properties of Solid Polymers*, 2nd ed.; J. Wiley & Sons: Chichester, U.K., 1983.
- (2) Treloar, L. R. G. *The Physics of Rubber Elasticity*, 3rd ed.; Clarendon Press: Oxford, U.K., 1975.

- (3) Hartwig, G. *Polymer Properties at Room and Cryogenic Temperature*; Plenum Press: New York, 1994.
- (4) Papkov, V. S.; Kvachev, Y. P. *Prog. Colloid Polym. Sci.* **1989**, *80*, 221.
- (5) Nakamae, K.; Nishino, T. In *Integration of Fundamental Polymer Science and Technology-5*; Lemstra, P. J., Kleintjens, L. A., Eds.; Elsevier Sci.: London, 1991, 121.
- (6) Nakamae, K.; Nishino, T. *Adv. X-ray Anal.* **1992**, *35*, 545.
- (7) Nakamae, K.; Nishino, T.; Gotoh, Y.; Matsui, R.; Nagura, M. *Polymer* **1999**, *40*, 4629.
- (8) Nishino, T.; Miyazaki, H.; Nakamae, K. *Rev. Sci. Instrum.* **2002**, *73*, 1809.
- (9) Kotera, M.; Nakai, A.; Saito, M.; Izu, T.; Nishino, T. *Polym. J.* **2007**, *39*, 1295.
- (10) Nakamura, C. E.; Whited, G. M. *Current Opin. Biotechnol.* **2003**, *14*, 454.
- (11) Zhang, J. J. *Appl. Polym. Sci.* **2004**, *91*, 1657.
- (12) Jakeways, R.; Ward, I. M.; Wilding, M. A.; Hall, I. H.; Desborough, I. J.; Pass, M. G. *J. Polym. Sci., Polym. Phys. Ed.* **1975**, *13*, 799.
- (13) Ward, I. M.; Wilding, M. A.; Brody, H. J. *Polym. Sci., Polym. Phys. Ed.* **1976**, *14*, 263.
- (14) Wu, J.; Schultz, J. M.; Samon, J. M.; Pangelinan, A. B.; Chuah, H. H. *Polymer* **2001**, *42*, 7161.
- (15) Nakamae, K.; Nishino, T.; Hata, K.; Yokoyama, F.; Matsumoto, T. *J. Soc. Mater. Sci., Jpn.* **1986**, *33*, 1066.
- (16) Nakamae, K.; Nishino, T.; Ohkubo, H.; Matsuzawa, S.; Yamaura, K. *Polymer* **1992**, *33*, 2581.
- (17) Nakamae, K.; Nishino, T.; Hata, K.; Matsumoto, T. *Kobunshi Ronbunshu* **1987**, *44*, 421.
- (18) Nishino, T.; Yokoyama, F.; Nakamae, K.; Matsumoto, T. *Kobunshi Ronbunshu* **1983**, *40*, 357.
- (19) Tashiro, K. *Prog. Polym. Sci.* **1993**, *18*, 377.
- (20) Yano, O.; Yamaoka, H. *Prog. Polym. Sci.* **1995**, *20*, 585.
- (21) Kalakkunnath, S.; Kalika, D. S. *Polymer* **2006**, *47*, 7085.
- (22) Chuah, H. H.; Lin-Vien, D.; Soni, U. *Polymer* **2001**, *42*, 7137.
- (23) Tadokoro, H. *Structure of Crystalline Polymers*; J. Wiley & Sons: New York, 1979.
- (24) Jeong, Y. G.; Bae, W. J.; Jo, W. H. *Polymer* **2005**, *46*, 8297.
- (25) Chuah, H. H. *Polym. Eng. Sci.* **2001**, *41*, 308.
- (26) Poulin-Dandurand, S.; Perez, S.; Revol, J.-F.; Brisse, F. *Polymer* **1979**, *20*, 419.
- (27) Desborough, I. J.; Hall, I. H.; Neisser, J. Z. *Polymer* **1979**, *20*, 545.
- (28) Ho, R.-M.; Ke, K.-Z.; Chen, M. *Macromolecules* **2000**, *33*, 7529.
- (29) Wang, B.; Li, C. Y.; Hanzlicek, J.; Cheng, S. Z. D.; Geil, P. H.; Grebowicz, J.; Ho, R.-M. *Polymer* **2002**, *42*, 7171.
- (30) Yang, J.; Sidoti, G.; Geil, P. H.; Li, C. Y.; Cheng, S. Z. D. *Polymer* **2001**, *42*, 7181.
- (31) Yokouchi, M.; Sakakibara, Y.; Chatani, Y.; Tadokoro, H.; Tanaka, K.; Yoda, K. *Macromolecules* **1976**, *9*, 266.
- (32) Nakamae, K.; Nishino, T.; Yokoyama, F.; Matsumoto, T. *J. Macromol. Sci.—Phys.* **1988**, *B27*, 407.
- (33) Jang, S. S.; Jo, W. H. *Fibers Polym.* **2000**, *1*, 18.
- (34) Kim, K. J.; Bae, J. H.; Kim, Y. H. *Polym. Int.* **2003**, *52*, 35.
- (35) Kaji, K.; Sakurada, I. *Makromol. Chem., Suppl.* **1975**, *1*, 599.
- (36) Nakamae, K.; Kameyama, M.; Yoshikawa, M.; Matsumoto, T. *Sen'I Gakkaishi* **1980**, *36*, T-33.